Astrochemistry: Recent Successes and Current Challenges
Proceedings IAU Symposium No. 231, 2005
D.C. Lis, G.A. Blake & E. Herbst, eds.

doi:10.1017/S1743921306007289

Molecular Gas at High Redshift

Pierre Cox

IRAM, 30 rue de la piscine, F-38406 Saint-Martin-d'Hères, France
email: cox@iram.fr

Abstract. The study of the molecular gas in quasars and submillimeter galaxies at high redshift has significantly progressed during the last few years. From the current detection of CO emission in 37 sources spanning a range in redshift from $1 < z < 6.4$ with, in some cases, the measurement of a series of CO rotational transitions, it is possible to constrain the physical conditions of the massive ($\geqslant 10^{10}\ M_\odot$) reservoirs of gas in these objects. This review will present the current status of the studies of molecular gas in high-z sources, detail the physical conditions which pertain in these systems, which are scaled-up versions of the local ULIRGS, and discuss the searches in high-z sources for species other than CO, including the fine structure lines of neutral carbon and the recent detection of the redshifted [C II] emission line in the $z = 6.4$ quasar J 1148+5251. These results hold great promise for the study of galaxy formation and their evolution with redshift. This review will conclude by outlining the expected progress in the field, in particular when future instruments such as ALMA will be operational, which will enable to study the astrochemistry and its evolution in the early universe.

Keywords. galaxies: high-redshift — galaxies: starburst — galaxies: ISM — cosmology: observations

1. Introduction

During the past decade, significant progress has been made in our knowledge of high-redshift ($z > 1$) galaxies through the study of the dense and warm molecular gas. Deep surveys and targeted observations of known galaxies and quasars done at millimeter and submillimeter wavelengths have revealed at high-z a population of objects with luminosities in excess of $10^{12}\ \mathrm{L}_\odot$, which is are scaled-up versions of the local ultraluminous infrared galaxies (ULIRGs) – see, *e.g.*, Blain *et al.* (2002), Sanders & Mirabel (1996). In these high-z galaxies and quasars, the far-infrared (far-IR) luminosity is mainly related to the warm ($40-60\,\mathrm{K}$) dust, with estimated dust masses of a few $10^8\ \mathrm{M}_\odot$, *e.g.*, Omont *et al.* (2001), Omont *et al.* (2003). The heating of the warm dust appears to be dominated by the starburst activity (rather than by an active galactic nucleus) with implied star formation rates of $\sim 1000\,\mathrm{M}_\odot\,\mathrm{yr}^{-1}$. It has been suggested that this population represents large spheroidal galaxies in the making (Blain *et al.* 2002), and the high star formation rates indicate that most of the stars could be formed in about 10^8 yr.

In a growing number of cases, warm and dense molecular gas has been detected in these high-z infrared luminous objects. Most of the observations were done via the detection of CO emission lines revealing giant reservoirs of molecular gas, with masses in excess of $10^{10}\ \mathrm{M}_\odot$, which provide the fuel needed to sustain the star-forming activity in these extreme objects. Recently, species other than CO, including rotational lines of hydrogen cyanide and fine-structure lines of neutral and singly-ionized carbon, have been used to probe the molecular gas in these high-z galaxies, providing additional information on the properties of the dense and warm interstellar medium in the early universe.

The detection of these often weak lines has been made possible by the increase in sensitivity of millimeter-wave telescopes, and is facilitated by a negative K-correction for the line emission and, for many of the source, by gravitational amplification. A recent review on molecules at high redshift has been given by Solomon & Vanden Bout (2005). In this paper, we review the recent advances which have been made in our understanding of the molecular gas content in high-z galaxies and summarize the prospects of these studies in view of future instruments, in particular with the Atacama Large Millimeter Array (ALMA).

2. CO Rotational Lines

IRAS F10214, an ultraluminous galaxy which was detected by IRAS, was the first high-z galaxy wherein CO line emission was discovered (Brown & Vanden Bout 1992; Solomon *et al.* 1992). This discovery prompted further searches and the successful detection of CO line emission in two high-z quasars: the Cloverleaf at $z = 2.5$ by Barvainis *et al.* (1994) (see also Barvainis *et al.* 1997) and BR 1202 at $z = 4.7$ by Omont *et al.* (1996). For both quasars, the CO emission was resolved (Fig. 1). Since then many more searches have been made and the molecular gas has now been measured in 37 high-z objects via the detection of rotational lines of CO (Table 1). The sources include far-IR ultraluminous ($> 10^{12}\,\mathrm{L}_\odot$) radio and submillimeter galaxies, quasars and one Lyman Break galaxy. The objects are in the redshift range $1 < z < 6.4$ and about half of them are gravitationally amplified (Table 1; see also Beelen *et al.* 2004; Greve *et al.* 2005; and Solomon & Vanden Bout 2005).

All the high-z galaxies detected in the CO line emission have CO luminosities in excess of $10^{10}\,\mathrm{K\,km\,s^{-1}\,pc^2}$, a factor of a few greater than for local ULIRGs, and the masses of the molecular gas reservoirs are of the order a few $10^{10}\,\mathrm{M}_\odot$. In the few cases where the sources have been resolved and where dynamical masses could be derived, the values are in the range of a few $10^{11}\,\mathrm{M}_\odot$, implying very massive systems, dominated by baryons in their central regions.

The correlation between the CO luminosity ($L'_{\mathrm{CO}(1\rightarrow0)}$) and L_{FIR} which is seen in nearby ULIRGs (*e.g.*, Solomon *et al.* 1997) is still valid for the high-z sources out to far-IR luminosities in excess of $10^{13}\,\mathrm{L}_\odot$. However, at the highest far-IR luminosities there is a clear trend in the sense of larger far-IR luminosity (or star formation rate) for a given CO luminosity (or a given mass of molecular gas) – see Figure 2. It appears therefore that for the infrared ultraluminous massive systems, which were present in the early universe, the star-formation efficiency (star-formation rate per unit gas mass) was higher than in the less luminous local ULIRGs (see, *e.g.*, Solomon *et al.* 1997).

Most of the high-z sources which were detected in the CO line emission are sources already known from optical or radio surveys. In contrast, the search for CO emission in submillimeter galaxies (SMGs) found in blind millimeter/submillimeter surveys has been less successful. The main reason is due to the fact that the objects are extremely faint in the optical making reliable redshift determinations very difficult. Until recently, only two SMGs were detected in CO (Frayer *et al.* 1998; Genzel *et al.* 2003). A major breakthrough was made by Chapman *et al.* (2003) who initiated a major observational program at the Keck Telescope to obtain spectroscopic redshifts for a large (∼70) sample of SMGs whose accurate positions were derived from deep VLA 1.4 GHz radio observations. Follow-up observations using the IRAM plateau de Bure interferometer successfully detected a large sub-sample of SMGs, bringing up to 12 the number of objects with CO detections (Neri *et al.* 2003; Greve *et al.* 2005). In some cases, higher angular resolution observations were able to resolve the CO line emission of the SMGs (Genzel *et al.* 2003; Tacconi *et al.* 2006).

From these observations, it is possible to derive the bulk properties of the SMG population. The median molecular gas mass is $\langle M(\mathrm{H}_2)\rangle = (3.0 \pm 1.6) \times 10^{10}\,M_\odot$ and

Table 1. High-z Quasars and Galaxies detected in the CO line emission

Source Name	z	Telescopes	CO Line line	CO Line [$\mathrm{Jy\,km\,s^{-1}}$]	1.2 mm Cont. [mJy]	Ref.
IRAS 10214+4724	2.28	12-m; 30-m	3→2	4.1±0.9	9.6±1.4	[1,2]
Cloverleaf	2.56	PdB; 30-m	3→2	9.9±0.6	18±2	[3]
BR 1202−0725	4.69	PdB; NRO	5→4	2.4±0.3	12.6±2.3	[4,5]
BRI 1335−0417	4.41	PdB	5→4	2.8±0.3	10.3±1.0	[6]
53W002	2.39	OVRO; PdB	3→2	1.20±0.15	1.7±0.4	[7,8]
MG 0414+0534	2.64	PdB	3→2	2.6±0.4	40±2†	[9]
SMM J02399−0136	2.80	OVRO; PdB	3→2	3.1±0.4	7.0±1.2	[10,11]
APM 08279+5255	3.91	PdB	4→3	3.7±0.5	17.0±0.5	[12]
BRI 0952−0115	4.43	PdB	5→4	0.91±0.11	2.8±0.6	[13]
Q1230+1627B	2.74	PdB	3→2	0.80±0.26	2.7±0.6	[13]
SMM J14011+0252	2.57	OVRO	3→2	2.4±0.3	≈ 3	[14]
4C60.07	3.79	PdB	4→3	2.50±0.43	4.5±1.2	[15]
6C1909+722	3.53	PdB	4→3	1.62±0.30	< 3	[15]
HR 10	1.44	PdB	5→4	1.35±0.20	4.9±0.8	[16]
MG 0751+2716	3.20	PdB	4→3	5.96±0.45	6.7±1.3	[17]
PSS 2322+1944	4.12	PdB	4→3	4.21±0.40	9.6±0.5	[18]
B3 J2330+3927	3.09	PdB	4→3	1.3±0.3	4.2±0.6	[19]
TN J0121+1320	3.52	PdB	4→3	1.2±0.4		[20]
J 1409+5628	2.56	PdB	3→2	3.28±0.36	10.7±0.6	[21]
J 1148+5251	6.42	VLA & PdB	3→2	0.18±0.04	5± 0.6	[22,23]
SMM J04431+0201	2.51	PdB	3→2	1.4±0.2	1.1±0.3	[24]
SMM J09431+4700	3.34	PdB	4→3	1.1±0.1	2.3±0.4	[24]
SMM J16358+4057	2.38	PdB	3→2	2.3±1.2	2.6±0.2	[24]
cB58	2.73	PdB	3→2	0.37±0.08	1.06±0.35	[25]
Q0957+561	1.41	PdB	2→1	1.20±0.06	5.7±1.8†	[26,27]
RX J0911+0551	2.79	OVRO	3→2	2.9±1.1	10.2±1.8	[28]
SMM J04135+1027	2.84	OVRO	3→2	5.4±1.3	7±1	[28]
B3 J2330+3927	3.08	PdB	4→3	1.3±0.3	4.8±1.2	[29]
4C41.17	3.79	PdB	4→3	1.8±0.2	3.8±0.4	[30]
TNJ0121+1320	3.52	PdB	4→3	1.2±0.4	–	[31]
TNJ0924−2201	5.19	ATCA	1→0	0.52±0.11	–	[32]
SMM J02396−0134	1.06	PdB	2→1	3.4±0.3	–	[33]
SMM J13120+4242	3.41	PdB	4→3	1.7±0.3	–	[33]
SMM J16366+4105	2.45	PdB	3→2	1.8±0.3	–	[33]
SMM J16371+4053	2.38	PdB	3→2	1.0±0.2	–	[33]
SMM J22174+0015	3.09	PdB	3→2	0.8±0.2	–	[33]
SMM J16359+6612	2.51	PdB & OVRO	3→2	5.75±0.25	3.0±0.7	[34]

References – [1] Brown & Vanden Bout (1992); [2] Solomon *et al.* (1992); [3] Barvainis *et al.* (1994); [4] Omont *et al.* (1996); [5] Ohta *et al.* (1996); [6] Guilloteau *et al.* (1997); [7] Scoville *et al.* (1997); [8] Alloin *et al.* (2000); [9] Barvainis *et al.* (1998); [10] Frayer *et al.* (1998); [11] Genzel *et al.* (2003); [12] Downes *et al.* (1999); [13] Guilloteau *et al.* (1999); [14] Frayer *et al.* (1998); [15] Papadopoulos *et al.* (2000); Andreani *et al.* (2000); [17] Barvainis *et al.* (2002); [18] Cox *et al.* (2002); [19] deBreuck *et al.* (2003); [20] deBreuck *et al.* (2003); [21] Beelen *et al.* (2004a); [22] Walter *et al.* (2003); [23] Bertoldi *et al.* (2003b); [24] Neri *et al.* (2003); [25] Baker *et al.* (2004); [26] Planesas *et al.* (1999); [27] Krips *et al.* (2005); [28] Hainline *et al.* (2004); [29] deBreuck *et al.* (2004a); [30] de Breuck *et al.* (2005); [31] deBreuck *et al.* (2004b); [32] Klamer *et al.* (2005); [33] Greve *et al.* (2005); [34] Kneib *et al.* (2005); Sheth *et al.* (2004).
Sources in bold face are known to be lensed.
† Non-thermal emission.

is distributed within a ∼2 kpc radius, with a median dynamical mass of $\langle M_{dyn} \rangle \simeq (1.2 \pm 1.5) \times 10^{11}\,\mathrm{M_\odot}$. The corresponding star formation rates are $\sim 700\,\mathrm{M_\odot\,yr^{-1}}$. These values are about four times greater than for local ULIRGs but similar to the most

https://doi.org/10.1017/S1743921306007289 Published online by Cambridge University Press

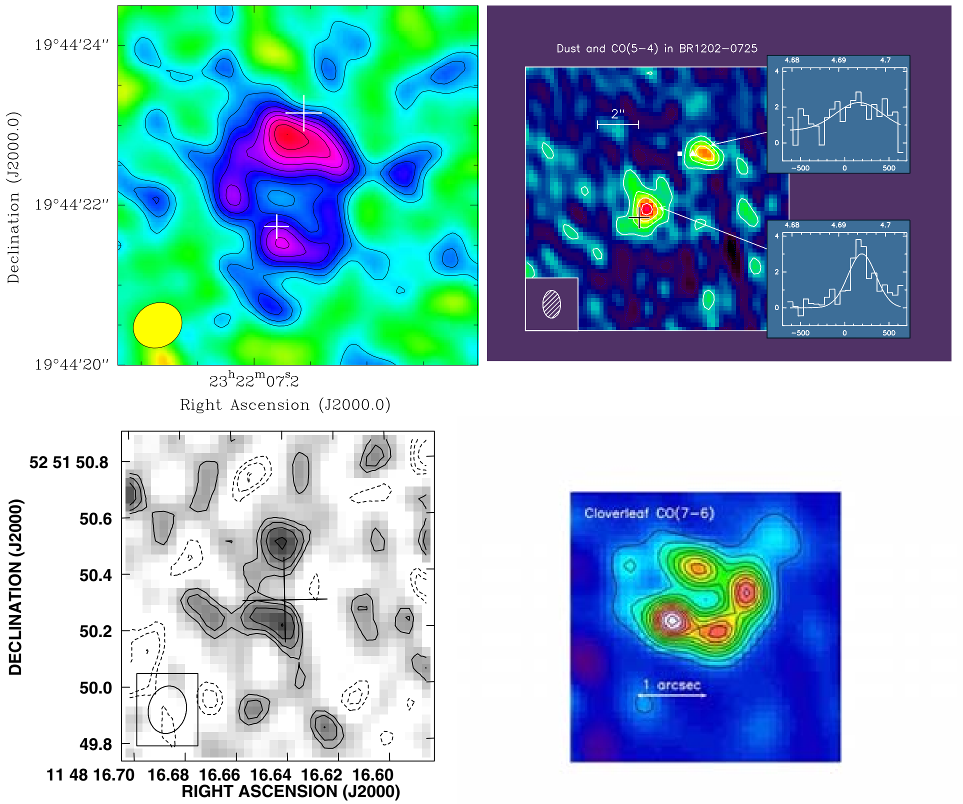

Figure 1. Examples of resolved CO emission in $z > 4$ QSOs. *From top to bottom and clockwise*: PSS 2322+1944 at $z = 4.12$ Carilli *et al.* (2003); BR 1202−0115 at $z = 4.69$ Omont *et al.* 1996; the Cloverleaf at $z = 2.6$ Alloin *et al.* (1997); J1148+5251 at $z = 6.42$ Walter *et al.* (2004).

extreme high-z radio galaxies and quasars. The CO line emission of the SMGS are broad ($\langle \text{FWHM} \rangle = 780 \pm 320\,\text{km}\,\text{s}^{-1}$) and display a high variety of profiles with, in many cases, double-peaked line profiles indicating merging systems or disks. The compactness of the sources and their properties show that the SMGs resemble scaled-up and more gas-rich versions of the ULIRGs in the local universe. Their masses, central densities and potential well depths are comparable to ellipticals galaxies or massive bulge. SMGs appear to convert most of the available initial gas into stars on typical time scales of a few $\sim 10^8$ yr.

In a few cases, the CO line emission in high-z galaxies has been resolved and Figure 1 presents four cases of resolved CO emission in high-z quasars. The properties of these four quasars are summarized below.

(a) The gravitationally lensed quasar PSS 2322+1944 at $z = 4.12$ reveals an Einstein ring with a diameter of 1.5″ which can be modeled as a star forming disk surrounding the QSO nucleus with a radius of 2 kpc (Carilli *et al.* 2003).

(b) The CO emission of BRI 1202−0115, a quasar at $z = 4.69$, is resolved into two sources (Omont *et al.* 1996; Carilli *et al.* 2002). The optical quasar is associated with the southern south. The CO line profiles and continuum levels are slightly different for the northern and southern sources indicating a system in the process of merging rather than gravitational lensing. Follow-up observations are still needed to confirm this result.

https://doi.org/10.1017/S1743921306007289 Published online by Cambridge University Press

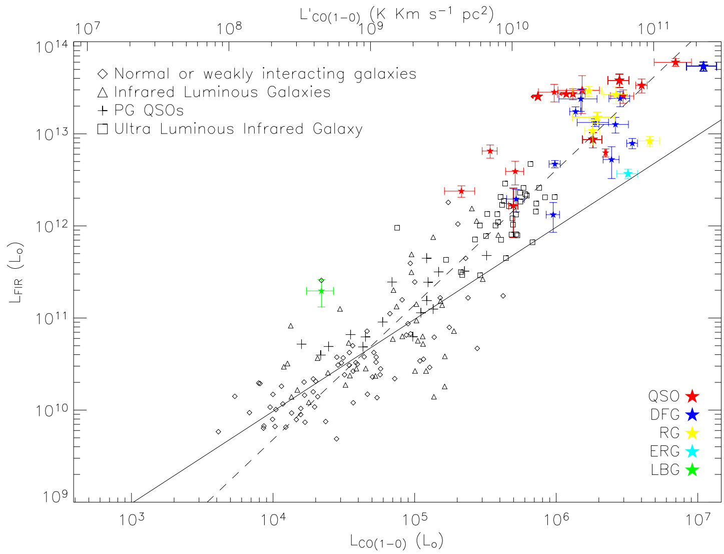

Figure 2. The correlation between the far-IR (L_{FIR}) and the CO ($L'_{\mathrm{CO}(1\to0)}$) luminosities for high-z galaxies and quasars (shown as stars and taken from Table 1), compared to local sources. The PG quasars are from Evans *et al.* (2001), Casoli & Loinard (2001) and Scoville *et al.* (2003), and the ULIRGS from Solomon *et al.* 1997. The sample of infrared luminous galaxies is taken from Yao *et al.* (2003) and the normal and the weakly interacting galaxies sample from Solomon & Sage (1988). The solid line shows the linear fit between L_{FIR} and $L'_{\mathrm{CO}(1\to0)}$ derived for sources with $L_{\mathrm{FIR}} < 10^{11}\,\mathrm{L}_\odot$. The dashed line displays the best fit to all the sources. This figure is taken from Beelen (2004b).

(*c*) The Cloverleaf (H1413+117), which is a strongly magnified quasar at $z = 2.5$, has the highest line flux densities of all high-z objects and hence has been observed in great detail. The high angular image (0.5″) clearly resolves the four 'leaves' of the Cloverleaf, which are similar to the optical image (Alloin *et al.* 1997). The radius of the CO emitting region is estimated to be 100 pc and the magnification is about 30.

(*d*) J1148+5251, the most distant quasar currently known at a redshift $z = 6.419$, is an extremely luminous quasar ($L_{\mathrm{bol}} \sim 10^{14}\,\mathrm{L}_\odot$) powered by a super-massive ($\approx 3\times10^9\,\mathrm{M}_\odot$) black hole. The detection of thermal dust emission in J 1148+5251 implies a dust mass of $\sim7\times10^8\,\mathrm{M}_\odot$, $L_{FIR} \sim 10^{13}\,\mathrm{L}_\odot$, and a corresponding star formation rate of $\sim2000\,\mathrm{M}_\odot\,\mathrm{yr}^{-1}$ (Bertoldi *et al.* 2003a). Three transitions of CO (J=3→2, 6→5, and 7→6) were detected in J1148+5251 (Walter *et al.* 2003; Bertoldi *et al.* 2003b). The molecular gas, with an estimated mass $\approx (1-2)\times10^{10}\,M_\odot$, is dense ($\sim10^5$ cm^{-3}) and warm (∼100 K). The gas mass detected in J 1148+5251 can fuel star formation at the rate implied by the far-infrared luminosity for only 10 million years, a time comparable to the dynamical time of the region. The gas must therefore be replenished quickly, and metal and dust enrichment must occur fast.

Walter *et al.* (2004) resolved the CO emission in J1148+5251 using the VLA: the molecular gas is extended to a radius of 2.5 kpc, and two peaks are seen in the central region, separated by 0.3″ (1.7 kpc), each containing $\sim5\times10^9\,\mathrm{M}_\odot$. The dynamical mass is estimated to be $\sim4.5\times10^{10}\,\mathrm{M}_\odot$, accounting for nearly all of the molecular gas. It is much smaller than what would be expected on the basis of the local $M_{BH}-\sigma_{bulge}$ relationship (Gebhardt *et al.* 2000), which predicts a halo of mass $\sim10^{12}\,\mathrm{M}_\odot$, if this relation is also valid at high redshifts.

https://doi.org/10.1017/S1743921306007289 Published online by Cambridge University Press

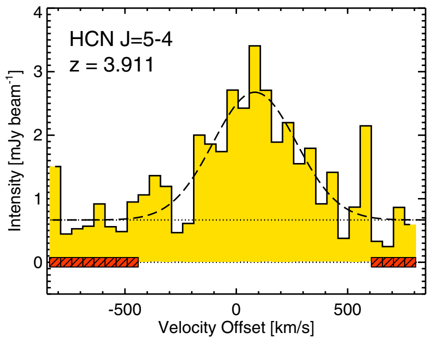

Figure 3. Spectrum of HCN(5→4) emission from the ultraluminous quasar APM08279+5255 at $z = 3.91$. The dashed line shows a Gaussian fit and the hatched regions indicate the channels sampling the continuum (from Wagg *et al.* 2006).

Finally, in a few cases it has been possible to observed in high-z galaxies various transitions of the CO rotational ladder. These measurements allow one to analyze the CO excitation and to better constrain the physical conditions of the molecular gas. A recent example of such a study is given by the observations of the strongly lensed SMG SMM 16359+6612 at $z = 2.5$ (Weiß *et al.* 2005b). Four CO lines are detected in SMM 16359+6612, namely J=3→2, 4→3, 5→4 and 6→5. The CO line spectral energy distribution (flux density *vs.* rotational quantum number) turns over at the CO(5→4) transition and is compatible with a gas density of $n_{\mathrm{H}_2} = 10^{3.4}\,\mathrm{cm}^{-3}$ and a kinetic temperature $T_{\mathrm{kin}} = 40\,\mathrm{K}$. Other galaxies have been found to be more excited with turn overs at higher rotational quantum numbers (6→5 and even 7→6) such as in BR 1202–0725 or the Cloverleaf.

3. Hydrogen Cyanide

Hydrogen cyanide (HCN), which has a higher dipole moment than CO, traces dense gas (the critical density for excitation of the lower order transitions is $n_{\mathrm{H}_2} \sim 10^5\,\mathrm{cm}^{-3}$) and is therefore better suited to probe the dense, warm gas directly associated with active star formation. Local ($z < 0.3$) ULIRGs show strong HCN emission (Gao & Solomon 2004) and display a tight linear relationship between the HCN luminosity (measuring the mass of dense gas available to make stars) and the far-IR luminosity (Fig. 4). This linear relationship indicates that the rate at which stars form is linearly proportional to the mass of *dense* molecular gas (Gao & Solomon 2004) as traced by HCN but not to the total molecular mass as traced by CO.

The potential to use HCN as a tracer of star formation activity in high-z sources has been demonstrated recently with the detection of HCN in four objects: the HCN(1→0) emission line is reported in the Cloverleaf at $z = 2.6$ (Solomon *et al.* 2003), in F10214 at $z = 2.3$ (Vanden Bout *et al.* 2004), and in the quasar J1409+5628 at $z = 2.6$ (Carilli *et al.* 2005); recently, the HCN(5→4) emission line was reported in the ultraluminous quasar APM08279+5255 at $z = 3.9$ by Wagg *et al.* (2006) – see Figure 3. Upper limits are available for four other high-z sources (see Carilli *et al.* 2005 and references therein). For all these source, the values of HCN/far-IR luminosity ratios are within the scatter of the relationship between HCN and far-IR emission for the $z < 0.3$ star-forming galaxies (Fig. 4) with values in between 1700 and 5000. The corresponding masses of dense molecular gas correspond to a few $10^{10}\,M_{\odot}$.

https://doi.org/10.1017/S1743921306007289 Published online by Cambridge University Press

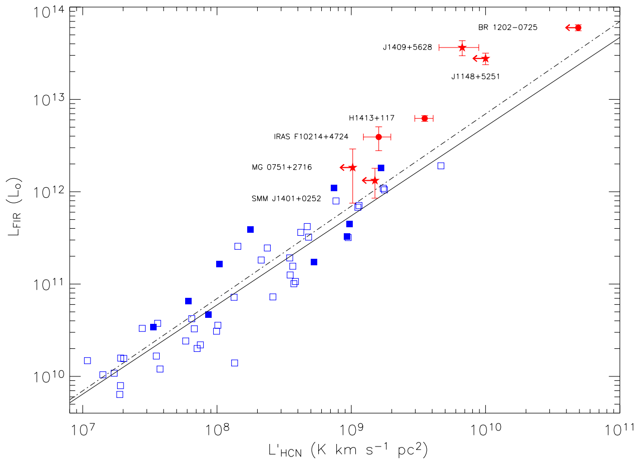

Figure 4. A comparison of the HCN line luminosity with far-IR luminosity for a sample of low-z galaxies (open squares from Gao & Solomon 2004a and filled squares from Solomon *et al.* 1992) and for high-z quasars and galaxies. The solid line is the nearly linear relationship defined by the low-z galaxies, corresponding to $\log L_{FIR} = 1.09 \log L_{\mathrm{HCN}} + 2.0$ (from Carilli *et al.* 2005).

4. Atomic Carbon: [C I] and [C II]

Atomic carbon is an important tracer of the dense molecular gas in external galaxies and plays a central role in the cooling of the gas (Gerin & Phillips 1998, 2000). In recent years, the fine structure lines of [C I] have been reported in high-z sources providing further constraints on the physical conditions of the interstellar gas (gas column densities, thermal balance, and the UV illumination) independently of CO studies.

Five high-z sources have now been detected in [C I] emission: the Cloverleaf, which has been detected in both fine-structure transitions (Barvainis *et al.* 1997 and Weiß *et al.* 2003, 2005b); the $z = 4.12$ quasar PSS2322+1944 (Pety *et al.* 2004); F10214 and the submillimeter $z = 2.5$ galaxy SMM14011+0252 (Weiß *et al.* 2005b); and recently the $z = 6.4$ quasar J1148+5251 (Bertoldi *et al.*, in preparation). In all cases, the line widths of the atomic carbon are similar to the CO widths, indicating that both species originate in the same volume. The inferred masses of neutral carbon are of the order of a few $10^7\,M_\odot$, and the carbon abundances are $\sim 3 - 5 \times 10^{-5}$, close to the galactic values, implying significant metal enrichment in heavy elements as early as $z \sim 2.5$.

The possibility of probing the interstellar medium and tracing star formation in galaxies at cosmological distances by using the bright C^+ emission line, when redshifted into submillimeter atmospheric windows, was proposed by Petrosian *et al.* (1969), and further discussed by Loeb (1993) and Stark (1997). The ${}^2P_{3/2} \rightarrow {}^2P_{1/2}$ fine-structure line of C^+ at 157.74 μm is the brightest emission line in the spectrum of galaxies, accounting for as much as ∼0.1–1% of their total luminosity. The line is emitted predominantly by gas exposed to ultraviolet radiation in photo-dissociation regions (PDRs) associated with star forming activity, and has been extensively used to investigate the physical conditions of PDRs and to trace star formation in local galaxies, see, *e.g.*, Malhotra *et al.* (2001). Deep searches were conducted in the recent years in $z > 3$ infrared luminous galaxies and quasars known to have massive reservoirs of molecular gas but have remained so far unsuccessful. The upper limits on the line intensities are consistent with the general decrease of the $L_{[CII]}/L_{FIR}$ ratio with increasing L_{FIR} beyond $10^{11.5}\,L_\odot$ which is observed for local ULIRGs (Fig. 5).

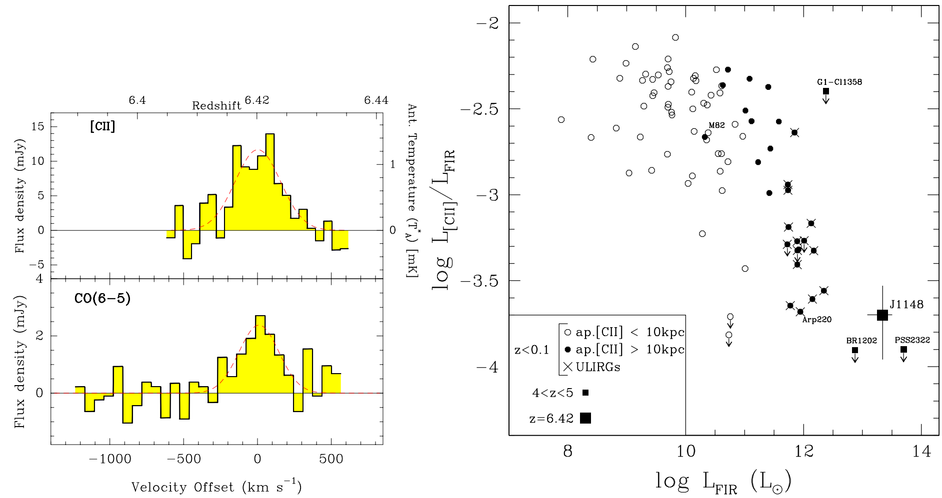

Figure 5. *Left panel*: Spectrum of the [C II] 157.74 μm emission line in the quasar J1148+5251 at $z = 6.42$ (*top panel*) compared to the CO(6→5) emission line. The dashed curves show the gaussian fits to the line profiles. *Right panel*: The $L_{[CII]}/L_{FIR}$ ratio versus L_{FIR} for normal and starburst local galaxies (circles) and for high-z sources (squares). J1148+5251 is shown with a large square. The small squares indicate the upper limits for the three other high-z sources where [C II] was searched for. Crosses indicate local ULIRGs ($L_{IR} > 10^{12}$ $L_\odot$). For reference, well-known local galaxies are also identified. From Maiolino *et al.* (2005).

Recently, Maiolino *et al.* (2005) reported the detection of the C^+ fine-structure line in the $z = 6.4$ quasar J1148+5251, using the IRAM 30-meter telescope (Fig. 5). The [C II] line has a luminosity of 4.4×10^9 $L_\odot$ and the $L_{[CII]}/L_{FIR}$ ratio is 2×10^{-4}, about an order of magnitude smaller than observed in local normal galaxies and similar to the ratio observed in local ULIRGs (Fig. 5). The detection of the [C II] line at high redshift suggests that the interstellar medium was already significantly enriched with metals at $z = 6.4$, i.e. when the universe was only 870 Myr old. This result shows the potential of using this emission line to investigate the star formation activity and the physics of the interstellar medium in the early universe.

5. Conclusions

The observations which are summarized in this review represent only the beginning of the study of the molecular gas associated with star-forming galaxies in the early universe. The data collected during the last decade have proven to be invaluable in constraining the physical characteristics (including the morphology, the masses, kinematics, densities and temperatures) of the massive reservoirs of dense and warm molecular gas from which the stars are formed when the universe was young, including the end of the reionization epoch (at $z = 5.4$.) The on-going and planned enhancements on some of the key operating facilities (such as the IRAM plateau de Bure interferometer, the Extended VLA or CARMA) will improve both on the sensitivity and the angular resolution, thereby enabling further detections and more detailed studies. It is likely that the samples of high-z for which information on the molecular gas will become available will further increase in the future and provide us with a better understanding of the processes which are involved in the formation of stars in early galaxies.

In the next decade, when ALMA will be fully operational, it will become possible to detect at submillimeter wavelengths high-z sources spanning the full range in luminosity from Milky Way type galaxies to the most massive systems in the universe. The superior sensitivity and spatial resolution of this array will enable to resolve many of the high-z sources in the CO line emission and to derive robust estimates of their dynamical masses, unhindered by extinction, thereby providing fundamental constraints to models of galaxy formation. It will also open up the possibility to detect, more routinely than today, atoms and molecules other than carbon monoxide, allowing us to probe the evolution of the chemistry and the abundances of molecular and atomic species in the early universe.

Acknowledgements

It is a pleasure to acknowledge collaborative work with F. Bertoldi, A. Omont, A. Beelen, C.L. Carilli & F. Walter which form the basis of the results presented in this paper. M. McClean is thanked for useful discussions related to molecular excitation. We are grateful to D. Lis for his nearly infinite patience in dealing with the delivery of this manuscript.

References

Alloin, D., Guilloteau, S., Barvainis, R., Antonucci, R., & Tacconi, L. 1997 *A&A* 321, 24
Alloin, D., Barvainis, R., & Guilloteau, S. 2000, *Ap. J.* 528, L81
Andreani, P., Cimatti, A., Loinard, L., & Röttgering, H. 2000, *A&A* 354, L1
Baker, A.J., Tacconi, L.J., Genzel, R., Lehnert, M.D., & Lutz, D. 2004, *Ap. J.* 604, 125
Barvainis, R., Tacconi, L., Antonucci, R., Alloin, D., & Coleman, P. 1994, *Nature* 371, 586
Barvainis, R., Maloney, P., Antonucci, R., & Alloin, D. 1997, *Ap. J.* 484, L13
Barvainis, R., Alloin, D., Guilloteau, S., & Antonucci, R. 1998, *Ap. J.* 492, L13
Barvainis, R., Alloin, D., & Bremer, M. 2002 *A&A* 385, 399
Beelen, A., Cox, P., Pety, J., Carilli, C.L., Bertoldi, F., *et al.* 2003, *A&A* 423, 441
Beelen, A. 2004, PhD thesis, Observatoire de Paris
Beelen, A., Cox, P, Benford, D., *et al.* 2005, *Ap. J.*, in press
Bertoldi, F. & Cox, P. 2002, *A&A* 884, L11
Bertoldi, F., Carilli, C.L., Cox, P., *et al.* 2003a, *A&A* 406, L55
Bertoldi, F., Cox, P., Neri, R., *et al.* 2003b, *A&A* 409, L47
Blain, A., Smail, I. Ivison, R., Kneib, J.-P., & Frayer, D. 2002, *Phys. Rep.* 369, 111
Brown, R.L. & Vanden Bout, P. 1992, *Ap. J.* 397, L11
Casoli, F. & Loinard, L. 2001, in: *Science with the Atacama Large Millimeter Array*, ed. A. Wootten (ASP Conf. Series, vol. 235), ∂. 305
Carilli, C.L., Bertoldi, F., Rupen, M.P., *et al.* 2001, *Ap. J.* 555, 625
Carilli, C.L., Kohno, K., Kawabe, R., *et al.* 2002, *A. J.* 123, 1838
Carilli, C.L., Lewis, G.F., Djorgovski, S.G., *et al.* 2003, *Science* 300, 773
Carilli, C.L., Solomon, P., Vanden Bout, P., *et al.* 2005, *Ap. J.* 618, 586
Chapman, S.C., Blain, A.W., Ivison, R.J., & Smail, I.R. 2003, *Nature* 422, 695
Cox, P. Omont, A., Djorgovski, S.G., *et al.* 2002, *A&A* 387, 406
de Breuck, C., Neri, R., Morganti, R., *et al.* 2003, *A&A* 401, 911
de Breuck, C., Bertoldi, F., Carilli, C.L., *et al.* 2004a, *A&A* 424, 1
de Breuck, C. Downes, D., Neri, R., van Breugel, W., Reuland, M., Omont, A., & Ivison, R. 2004b, *A&A*, 430, L1
De Breuck, C., Downes, D., Neri, R., van Breugel, W., Reuland, M., Omont, A., & Ivison, R. 2005, *A&A* 430, L1
Downes, D., Neri, R., Wiklind, T., Wilner, D.J., & Shaver, P.A. 1999, *Ap. J.* 513, L1
Evans, A.S., Frayer, D.T., Surace, J.A., & Sanders, D.B. 2001, *A. J.* 121, 1893
Fan, X., Hennawi, J.F., Richards, G., *et al.* 2004, *A. J.* 128, 515
Frayer, D.T., Ivison, R.J., Scoville, N.Z., Yun, M., Evans, A.S., Smail, I., Blain, A.W., & Kneib, J.-P. 1998, *Ap. J.* 506, L7
Gao, Y. & Solomon, P.M. 2004, *Ap. J.* 606, 271

Gebhardt, K., Bender, R., Dressler, A., *et al.* 2000, *Ap. J.* 539, L13
Genzel, R., Baker, A.J., Tacconi, L.J., Lutz, D., Cox, P., Guilloteau, S., & Omont, A. 2003, *Ap. J.* 584, 633
Gerin, M. & Phillips, T.G. 1998, *Ap. J.* 509, L17
Gerin, M. & Phillips, T.G. 2000, *Ap. J.* 537, 644
Guilloteau, S., Omont, A., McMahon, R.G., Cox, P., & Petitjean, P. 1997, *A&A* 328, L1
Guilloteau, S., Omont, A., Cox, P., *et al.* 1999, *A&A* 349, 363
Greve, T.R., Bertoldi, F., Smail, I. *et al.* 2005, *MNRAS* 359, 1165
Hainline, L.J., Scoville, N.Z., Yun, M.S., Hawkins, D.W., Frayer, D.T., & Isaak, K.G. 2004, *Ap. J.* 609, 61
Isaak, K.G., Priddey, R.S., McMahon, R.G. *et al.* 2002, *MNRAS* 329, 149
Kauffmann, G. & Haehnelt, M. 2000, *MNRAS* 311, 576
Kalmer, I.J., Ekers, R.D., Sadler, E.M., Weiß, A., Hunstead, R.W., & de Breuck, C. 2005, *Ap. J.* 621, L1
Kneib, J.-P., Neri, R., Smail, I., Blain, A., Sheth, K., van der Werf, P. & Knudsen, K.K. 2005, *A&A* 434, 819
Krips, M., Neri, R., Eckart, A., Downes, D., Martin-Pintado, J., & Planesas, P. 2005, *A&A* 431, 879
Loeb, A. 1993, *Ap. J.* 404, L37
Sanders, D.B. & Mirabel, I.F. 1996, *ARA&A* 34, 749
Maiolino, R., Cox, P., Caselli, P., *et al.* 2005, *A&A* 440, L51
Malhotra, S., *et al.* 2001, *Ap. J.* 561, 766
Neri, R., Genzel, R., Ivison, R.J., *et al.* 2003, *Ap. J.* 597, L113
Ohta, K., Yamada, T., Nakanishi, K., Kohno, K., Akiyama, M., & Kawabe, R. 1996, *Nature* 382, 426
Omont, A., Petitjean, P., Guilloteau, S., *et al.* 1996, *Nature* 382, 428
Omont, A., Cox, P., Bertoldi, F., *et al.* 2001, *A&A* 374, 371
Omont, A., Beelen, A., Bertoldi, F., *et al.* 2003, *A&A* 398, 857
Papadopoulos, P.P., Röttgering, H.J.A., van der Werf, P.P., Guilloteau, S., Omont, A., van Breugel, W.J.M., & Tilanus, R.P.J. 2000, *Ap. J.* 528, 626
Petrosian, V., Bahcall, J.N., & Salpeter, E.E. 1969, *Ap. J.* 155, L57
Pety, J., Beelen, A., Cox, P., *et al.* 2004, *A&A* 428, L21
Planesas, P., Martin-Pintado, J., Neri, R., & Colina, L. 1999, *Science* 286, 2493
Priddey, R.S., Isaak, K.G., McMahon, R.G., & Omont, A. 2003, *MNRAS* 339, 1183
Scoville, N.Z., Yun, M.S., Windhorst, R.A., Keel, W.C., & Armus, L. 1997, *Ap. J.* 485, L21
Scoville, N.Z., Frayer, D.T. Schinnerer, E., & Christopher, M. 2003, *Ap. J.* 585, L105
Sheth, K., Blain, A.W., Kneib, J.-P., Frayer, D.T., van der Werf, P.P., & Knudsen, K.K. 2004, *Ap. J.* 614, L5
Solomon, P.M. & Sage, L.J. 1988, *Ap. J.* 334, 613
Solomon, P.M., Downes, D., & Radford, S.J.E. 1992, *Ap. J.* 398, L29
Solomon, P.M., Downes, D., Radford, S.J.E, & Barrett, J.W. 1997, *Ap. J.* 478, 144
Solomon, P.M., Vanden Bout, P., Carilli, C.L., & Guélin, M. 2003, *Nature* 426, 636
Solomon, P.M. & Vanden Bout, P.A. 2005, *ARA&A* 43, 677
Stark, A.A. 1997, *Ap. J.* 481, 587
Tacconi, L.J., Neri, R., Chapman, S.C., Genzel, R., *et al.* 2006, *Ap. J.*, in press
Vanden Bout, P.A., Solomon, P.M., & Maddalena, R.J. 2004, *Ap. J.* 614, L97
Wagg, J., Wilner, D.J., Neri, R., Downes, D., & Wiklind, T. 2006, *Ap. J.*, in press
Walter, F., Bertoldi, F., Carilli, C., *et al.* 2003, *Nature* 424, 406
Walter, F., Carilli, C.L., Bertoldi, F., *et al.* 2004, *Ap. J.* 615, L17
Weiß, A., Henkel, C., Downes, D., & Walter, F. 2003, *A&A* 409, L41
Weiß, A., Downes, D., Henkel, C., & Walter, F. 2005a, *A&A* 249, L25
Weiß, A., Downes, D., Walter, F., & Henkel, C. 2005b, *A&A* 440, L45
Yao, L., Seaquist, E.R., Kuno, N., & Dunne, L. 2003, *Ap. J.* 597, 1271

https://doi.org/10.1017/S1743921306007289 Published online by Cambridge University Press